Light-scattering intensity on reversible cluster-cluster aggregations

1999 J. Phys.: Condens. Matter 11 7071

(http://iopscience.iop.org/0953-8984/11/37/304)

J. Phys.: Condens. Matter **11** (1999) 7071–7078. Printed in the UK PII: S0953-8984(99)04723-2

Light-scattering intensity on reversible cluster–cluster aggregations

Takamichi Terao and Tsuneyoshi Nakayama
Department of Applied Physics, Hokkaido University, Sapporo 060-8628, Japan
E-mail: terao@eng.hokudai.ac.jp

Received 2 June 1999

Abstract. We investigate the light-scattering intensity on three-dimensional cluster–cluster aggregations. The effect of reversible aggregation on the light-scattering intensity is clarified in terms of numerical simulations. For the case of weak interaction between particles, there is no peak as a function of the scattering wavenumber q in the static light-scattering intensity. We find that the profile of the light-scattering intensity on reversible cluster–cluster aggregations is apparently different from that for diffusion-limited cluster–cluster aggregations.

1. Introduction

The aggregation process of particles has attracted a great deal of interest in recent years, due to its wide range of practical applications and its scientific importance [1, 2]. The cluster–cluster aggregation model (CCA) was developed by Meakin [3] and Kolb, Botet and Jullien [4]; it describes the sol–gel transition due to a nonequilibrium process, the understanding of whose underlying mechanism, leading to the formation of gel networks, has remained far from complete. When the particle concentration c is larger than a characteristic gel concentration c_g, an aggregate spans a box from edge to edge and forms a gel network. Though several different models have been proposed to elucidate the formation of gel networks [5], the cluster–cluster aggregation model (CCA) is the most successful one as regards understanding the gel formation. This model produces clusters with scale invariance such as

$$M(R) \propto R^{D_f} \tag{1}$$

where $M(R)$ is a total mass of the cluster and D_f is its fractal dimension [3, 4]. There are two types of model, namely diffusion-limited cluster–cluster aggregation (DLCA) and reaction-limited cluster–cluster aggregation (RLCA), which correspond to fast and slow aggregation processes, respectively. Among the typical cluster–cluster aggregations are colloidal aggregations, and a lot of experimental work has been performed on these systems [6–9]. Among the studies, static light-scattering measurement is powerful for clarifying the structure of the aggregations, which gives us useful information such as the average radius of gyration. Gonzalez and Ramirez-Santiago have performed numerical simulations on the three-dimensional RLCA model [10, 11]. Their results have indicated that there is a peak at nonzero scattering vector q in the light-scattering intensity in the RLCA model, as well as in the DLCA model.

In this paper, we study numerically the static light-scattering intensity $I(q)$ on three-dimensional *reversible* cluster–cluster aggregation, which forms a physical gel network

0953-8984/99/377071+08$30.00

[12–14]. Provided that the effective attractive interactions between particles are relatively weak, particles have high probability of escaping from the cluster. In contrast to the ordinary cluster–cluster aggregation model, this aggregation process is reversible—particles are allowed to restructure within clusters or even break apart from them. In contrast to the case for the DLCA model, the physical properties of the reversible cluster–cluster aggregation model have not been clarified so far. In a previous study, we have numerically investigated the sol–gel transition using the reversible cluster–cluster aggregation model [14]. We calculate the time development of the light-scattering intensity $I(q)$ in the reversible cluster–cluster aggregation model, to clarify the effect of reversibility on the cluster formation [12–14]. In addition, the light-scattering properties of the irreversible cluster–cluster aggregations with different sticking probabilities between particles are given for comparison; this corresponds to the regime intermediate between the DLCA and RLCA. These results indicate a clear difference between $I(q)$ for reversible cluster–cluster aggregations and that for irreversible ones.

This paper is organized as follows. In section 2, we describe the detail of the cluster–cluster aggregation model. In section 3, the numerical results on the static light-scattering intensity on three-dimensional cluster–cluster aggregations are displayed. Section 4 is devoted to discussion and conclusions.

2. Models

We describe the formation rule for the cluster–cluster aggregation [15, 16]. We take the unit $a = 1$ for the lattice constant. In this model, N particles are randomly disposed in a cubic box of size L, where the particle concentration c becomes

$$c \equiv N/L^3. \tag{2}$$

The ith particle (or cluster) is chosen at random according to the probability $P(n_i, \alpha)$ defined by

$$P(n_i, \alpha) \equiv n_i^\alpha \Big/ \sum_i n_i^\alpha \tag{3}$$

where n_i is the number of particles in the ith cluster and α is a numerical parameter. In most studies, the value of α is taken as $\alpha = -1/D_f$, which is analogous to the diffusion constant of each cluster being inversely proportional to the gyration radius R_g [17, 18]. The ith cluster is moved by one step along a randomly chosen direction among six directions $(\pm 1, 0, 0)$, $(0, \pm 1, 0)$, $(0, 0, \pm 1)$ in a cubic box. If the cluster does not collide with another one, the displacement is performed and the algorithm goes on by choosing another cluster. If a collision occurs between two clusters, they stick together forming a new large cluster with a sticking probability p, and another cluster is chosen again at random.

Reversible cluster–cluster aggregations are described by modifying the diffusion-limited cluster–cluster aggregations with a finite interparticle attraction energy. The energy of interaction ϵ_{mn} between particles m and n is defined to be $\epsilon_{mn} = -\epsilon$ $(\epsilon > 0)$ if particles m and n are nearest neighbours; otherwise $\epsilon_{mn} = 0$. A particle is allowed to rearrange its position by one lattice unit within the same cluster or break away from it, according to the probability p_b:

$$p_b = \begin{cases} 1 & \text{for } \Delta E < 0 \\ \exp(-\Delta E/k_B T) & \text{for } \Delta E \geqslant 0 \end{cases} \tag{4}$$

where k_B, T and ΔE are the Boltzmann constant, the temperature of the system and the energy difference due to the unbinding of a particle, respectively. After sufficiently long time steps, the system reaches an equilibrium state. At finite temperature, the structure of

the aggregations does not become compact [12–14]. The properties of reversible cluster–cluster aggregations change on varying the ratio τ_R/τ_D, where $1/\tau_D$ and $1/\tau_R$ are the attempt frequency for diffusive motion of a cluster and that for particle rearrangement due to thermal fluctuations, respectively. When $\tau_R/\tau_D \gg 1$, the system is governed by the diffusive motion of clusters, which corresponds to irreversible aggregations. When $\tau_R/\tau_D \ll 1$, the properties of the system are solely determined by statistical equilibrium conditions. In such a case, the system becomes a sticky hard-sphere system; these have been extensively studied.

3. Numerical results

We have formed large-scale cluster–cluster aggregations by means of computer simulations. Periodic boundary conditions are employed in all spatial directions. In the following, we consider the case where $\tau_R/\tau_D = 1$, when the attempts at cluster diffusion and particle rearrangement are performed with the same frequency. This means that the effects of the diffusive motion of clusters (particles) and thermal fluctuations are both important in this system. Figure 1 shows a snapshot of $d = 3$ reversible cluster–cluster aggregations formed on a simple-cubic lattice, after sufficiently long time steps. In figure 1, the system size and the particle concentration are taken as $L = 40$ and $c = 0.05$, respectively, and the temperature is chosen to be $k_BT = 0.1\epsilon$. We can see that the maximum cluster spans from end to end in a box and forms a gel network. In these systems, there is a sol–gel transition as a function of particle concentration c and the temperature T, and the transition temperature decreases as the particle concentration becomes small [14]. The fractal dimension of these aggregations is known to be $D_f = 2.4 \pm 0.1$ [14]. For systems formed by monodisperse particles, the light-scattering intensity $I(q)$ is given by

$$I(q) = P(q)S(q) \tag{5}$$

where $P(q)$ is a form factor for spherical particles of unit diameter ($a = 1$) such as

$$P(q) = \left\{24\frac{\sin(q/2) - (q/2)\cos(q/2)}{q^3}\right\}^2 \tag{6}$$

and $S(q)$ is the structure factor which is related to the density–density correlation function by means of the Fourier transform [15, 19]. In the actual calculations, the structure factor $S(\boldsymbol{q})$ is

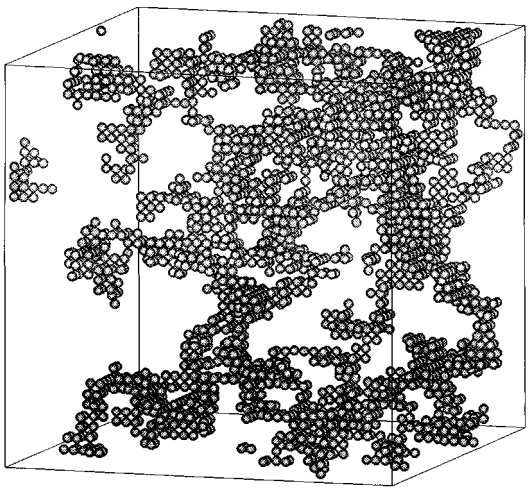

Figure 1. Three-dimensional reversible cluster–cluster aggregation on a simple-cubic lattice. The system size and the particle concentration are taken as $L = 40$ and $c = 0.05$, respectively. The temperature of the system is chosen to be $k_BT/\epsilon = 0.1$.

given by [20]

$$S(\boldsymbol{q}) \equiv \frac{1}{N}\sum_{m,n}\exp\{\mathrm{i}\boldsymbol{q}\cdot(\boldsymbol{r}_m-\boldsymbol{r}_n)\} = \frac{1}{N}\left|\sum_{m=1}^{N}\exp(\mathrm{i}\boldsymbol{q}\cdot\boldsymbol{r}_m)\right|^2 \tag{7}$$

where $\boldsymbol{r}_m$ and $\boldsymbol{q}$ are the positional vector of the mth particle and the scattering vector ($q \equiv |\boldsymbol{q}|$), respectively.

Figure 2 shows the time development of the static light-scattering intensity $I(q)$ on three-dimensional reversible cluster–cluster aggregation. The system size L, the particle concentration c and the temperature of the system are taken as $L = 80$, $c = 0.05$ and $k_BT/\epsilon = 1.0$, respectively, There is a gelling network spanning the whole system with these parameters [14]. The number of time steps n_t is chosen as $n_t = 1.2\times10^5$, 2.4×10^5, 3.6×10^5, 4.8×10^5, 6.0×10^5, 7.2×10^5 and 9.6×10^5. These results indicate that the peak intensity becomes larger and the peak position of the scattering intensity $q = q_{\max}$ shifts to lower q as the gelation proceeds. After long time steps ($n_t \geqslant 6.0\times10^5$), the peak of $I(q)$ vanishes. To our knowledge, this is the first study of the light-scattering intensity $I(q)$ on reversible cluster–cluster aggregations in computer simulations.

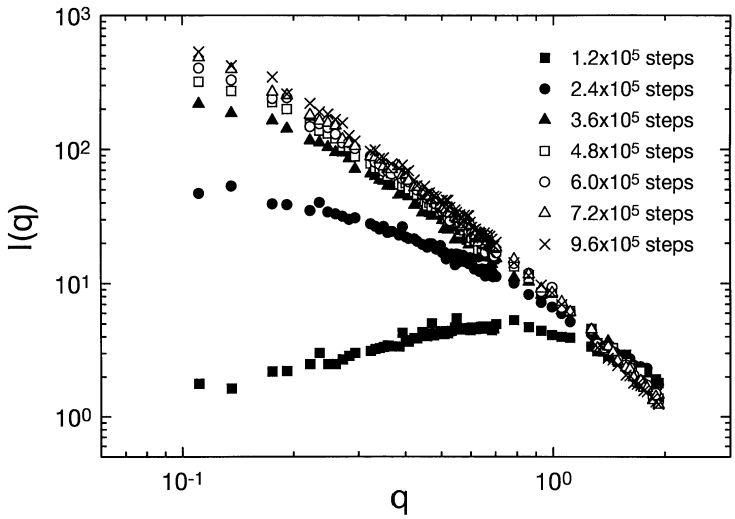

Figure 2. The static light-scattering intensity $I(q)$ of $d = 3$ reversible cluster–cluster aggregations. The system size L and the particle concentration c are taken as $L = 80$ and $c = 0.05$, respectively. The temperature of the system is chosen as $k_BT/\epsilon = 1.0$. The number of time steps n_t is chosen as $n_t = 1.2\times10^5$, 2.4×10^5, 3.6×10^5, 4.8×10^5, 6.0×10^5, 7.2×10^5 and 9.6×10^5.

We also show the profile of the light-scattering intensity $I(q)$ of irreversible cluster–cluster aggregations for comparison. There are two limiting regimes of the aggregation processes. One is a rapid regime called diffusion-limited cluster–cluster aggregation characterized by $D_f \approx 1.78$ in a three-dimensional system ($d = 3$), for which the colliding particles stick at first contact [15,21]. The other is a much slower regime, called reaction-limited cluster–cluster aggregation, due to a very small sticking probability caused by potential barriers between particles, leading to more compact clusters with, e.g., $D_f \approx 2.1$ for $d = 3$. The sticking probability p is chosen as $p = 1$ for the DLCA model [15] and $p \ll 1$ for the RLCA model [22]. In the irreversible aggregation, a single aggregate is formed after long time steps. Figure 3(a) shows the profiles $I(q)$ for $d = 3$ cluster–cluster aggregations with conditions intermediate

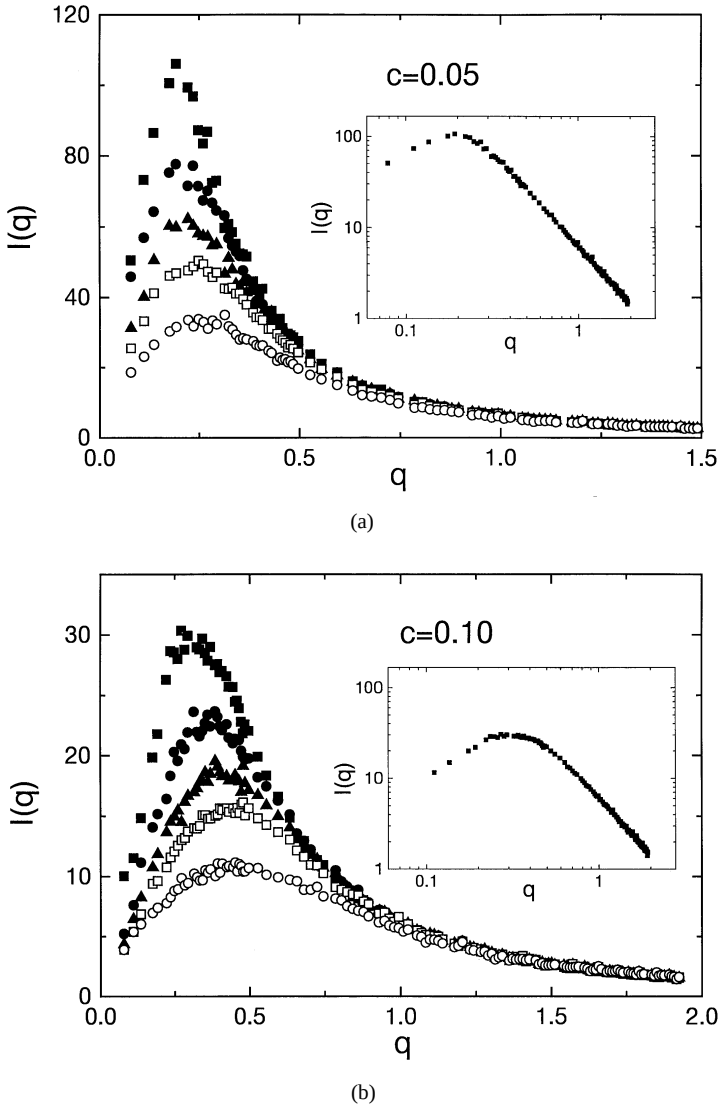

(a)

(b)

Figure 3. (a) The static light-scattering intensity $I(q)$ for $d = 3$ irreversible cluster–cluster aggregations. The system size L and the particle concentration c are taken as $L = 80$ and $c = 0.05$, respectively. Filled squares, filled circles, filled triangles, open squares and open circles correspond to the results for sticking probabilities $p = 0.02$, 0.05, 0.10, 0.20 and 1.0, respectively. The inset shows a logarithmic plot of $I(q)$ with $p = 0.02$. (b) The static light-scattering intensity $I(q)$ of $d = 3$ cluster–cluster aggregations. The particle concentration c is taken as $c = 0.10$. The inset shows a logarithmic plot of $I(q)$ with $p = 0.02$.

between those of the DLCA and RLCA models. The system size and the particle concentration of the aggregations in figure 3(a) are taken to be $L = 80$ and $c = 0.05$, respectively, and the ensemble average is taken over 120 samples. In figure 3(a), the results for sticking probabilities $p = 0.02$, 0.05, 0.10, 0.20 and 1.00 (DLCA) are shown, which corresponds to changing the potential barriers between particles in colloidal aggregations. Figure 3(b) shows the profiles $I(q)$ for $d = 3$ cluster–cluster aggregations with the particle concentration $c = 0.10$. In

figures 3(a) and 3(b), the existence of the peak at nonzero scattering vector $q = q_{\max}$ reflects the density fluctuations in the aggregation [10, 17]. With larger concentration c (figure 3(b)), the correlation length ξ of the system becomes smaller and the peak position $q = q_{\max}$ shifts to a higher-q regime, because the peak position $q = q_{\max}$ is inversely proportional to the correlation length of the aggregations ξ [15]. We observe that the peak position $q = q_{\max}$ shifts to lower q as the sticking probability p decreases. This suggests that the correlation length $\xi \approx 2\pi/q_{\max}$ becomes larger with decreasing sticking probability p. With $p = 0.02$, it is also confirmed that $I(q)$ obeys a power-law behaviour such as

$$I(q) \propto q^{-D_f} \qquad (D_f = 2.10 \pm 0.03) \tag{8}$$

within the regime $2\pi\xi^{-1} < q < 2\pi a^{-1}$ (see the insets of figures 3(a) and 3(b)).

Figure 4 shows the dependence on the sticking probability p of the peak intensity $I(q = q_{\max})$, with the particle concentrations $c = 0.05$ and 0.10. Figure 4 shows that the peak intensity increases with decreasing sticking probability p, which reflects the fact that the structure of the aggregation becomes more compact. These results show that there is a definite peak in the scattering intensity $I(q)$ in three-dimensional irreversible cluster–cluster aggregations, in agreement with previous studies [10, 11]. We confirm that the profiles of the light-scattering intensity $I(q)$ on the reversible cluster–cluster aggregations are apparently different from those for the irreversible ones such as the DLCA and RLCA [10, 11].

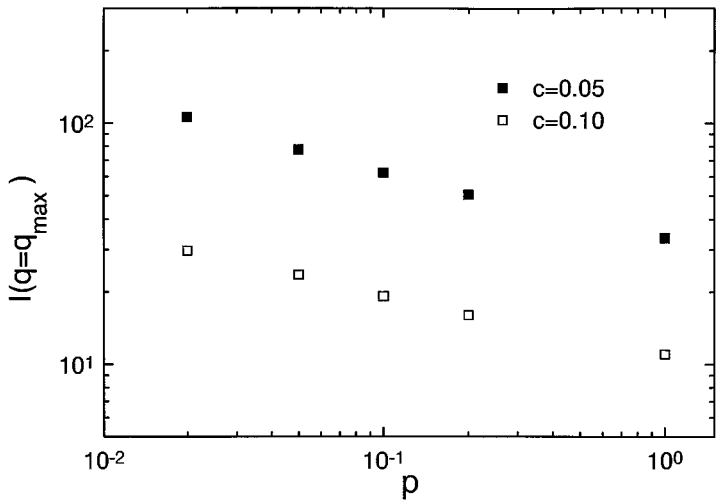

Figure 4. The dependence on the sticking probability p of the peak intensity $I(q = q_{\max})$. Solid squares and open squares display the results for $c = 0.05$ and 0.10, respectively.

4. Conclusions

We have performed computer simulations on three-dimensional reversible cluster–cluster aggregation. The profile of $I(q)$ for $d = 3$ reversible cluster–cluster aggregations has been studied numerically. After sufficiently long time steps, the scattering intensity $I(q)$ has no peak for reversible cluster–cluster aggregations in the observed q-regime. We also study the irreversible cluster–cluster aggregations [23, 24] for comparison, with different particle concentrations c and sticking probabilities p. It is found that there is a definite peak in the q-dependence of the scattering intensity $I(q)$ for $d = 3$ irreversible cluster–cluster aggregations,

in agreement with previous studies [10, 11]. We have shown that the peak intensity increases with decreasing sticking probability p, which reflects the fact that the structure of the clusters becomes more compact. These results clarify the light-scattering properties on reversible cluster–cluster aggregations, and that the profile of the light-scattering intensity $I(q)$ is different from that for the irreversible ones such as the DLCA and RLCA [10, 11]. There are several phenomenological formulae for the structure factor $S(q)$, based on the single-aggregate theory [15]. An example is the Fisher–Burford formula [17, 25]:

$$S(q) = S(0)\left\{1 + \frac{2}{3D_f}R_g^2 q^2\right\}^{-D_f/2} \tag{9}$$

in which there is no peak in the q-dependence. This suggests that the intercluster correlation is destroyed on reversible cluster–cluster aggregations (figure 2) due to thermal fluctuations.

For low salt concentrations, Coulomb repulsion between charged colloidal particles becomes relevant (no screening effect). This makes the effective attractive interactions between colloidal particles weak, where the interaction energy between colloidal particles becomes small ($\sim k_B T$). As a result, the effect of reversibility between neighbouring particles is not negligible. Most of the previous experiments with colloidal systems have been performed on the irreversible cluster–cluster aggregations, and those on the reversible cluster–cluster aggregations are fairly few [2, 6]. Detailed experimental studies are expected to confirm the relationship between the reversible aggregation processes and the experimental results on colloidal aggregations. To summarize, we have demonstrated that the analysis of the static light-scattering intensity is a powerful tool for studying the mechanism of the aggregation phenomena. This work will shed light on the interpretation of light-scattering experiments for dense colloidal aggregations.

Acknowledgments

The authors are grateful to the Supercomputer Centre, Institute of Solid State Physics, University of Tokyo for the use of the facilities. This work was supported in part by a Grant-in-Aid from the Japan Ministry of Education, Science and Culture for Scientific Research.

References

[1] Witten T A and Sander L M 1981 *Phys. Rev. Lett.* **47** 1400
[2] Vicsek T 1989 *Fractal Growth Phenomena* (Singapore: World Scientific)
[3] Meakin P 1983 *Phys. Rev. Lett.* **51** 1119
[4] Kolb M, Botet R and Jullien R 1983 *Phys. Rev. Lett.* **51** 1123
[5] Family F and Landau D P 1984 *Kinetics of Aggregation and Gelation* (Amsterdam: North-Holland)
[6] Robinson D J and Earnshaw J C 1992 *Phys. Rev.* A **46** 2045 and references therein
[7] Asnaghi D, Carpineti M, Giglio M and Vailati A 1995 *Physica* A **213** 148
[8] Aubert C and Cannel D S 1986 *Phys. Rev. Lett.* **56** 738
[9] Dimon P, Sinha S K, Weitz D A, Safinya C R, Smith G S, Varady W A and Lindsay H M 1986 *Phys. Rev. Lett.* **57** 595
[10] Gonzalez A E and Ramirez-Santiago G 1995 *Phys. Rev. Lett.* **74** 1238
[11] Ramirez-Santiago G and Gonzalez A E 1997 *Physica* A **236** 75
[12] Shih W Y, Aksay I A and Kikuchi R 1987 *Phys. Rev.* A **36** 5015
[13] Jin J-M, Parbhakar K, Dao L H and Lee K H 1996 *Phys. Rev.* E **54** 997
[14] Terao T and Nakayama T 1998 *Phys. Rev.* E **58** 3490
[15] Hasmy A, Anglaret E, Foret M, Pelous J and Jullien R 1994 *Phys. Rev.* B **50** 6006
[16] Terao T, Yamaya A and Nakayama T 1998 *Phys. Rev.* E **57** 4426
[17] Haw M D, Poon W C K and Pusey P N 1997 *Phys. Rev.* E **56** 1918
[18] Stauffer D and Aharony A 1992 *Introduction to Percolation Theory* 2nd edn (London: Taylor & Francis)

[19] Oh C and Sorensen C M 1998 *Phys. Rev.* E **57** 784
[20] Hasmy A, Foret M, Pelous J and Jullien R 1993 *Phys. Rev.* B **48** 9345
[21] Rahmani A, Benoit C, Jullien R and Poussigue G 1998 *Phil. Mag.* B **77** 421
[22] Brown W D and Ball R C 1985 *J. Phys. A: Math. Gen.* **18** L517
[23] Asnaghi D, Carpineti M, Giglio M and Sozzi M 1992 *Phys. Rev.* A **45** 1018
[24] Di Biasio A, Bolle G, Cametti C, Codastefano P, Sciortino F and Tartaglia P 1994 *Phys. Rev.* E **50** 1649
[25] Fisher M E and Burford R J 1967 *Phys. Rev.* B **156** 583